

Photosynthetic behavior of the grapevine 'Itália' in relation to water availability in protected cultivation

Leonardo Cury da Silva^{1,a}, Henrique Pessoa dos Santos², Flávio Bello Fialho², Gilmar Arduino Bettio Marodin³, Homero Bergamaschi³, Carlos Alberto Flores⁴ and Daniel Antunes Souza⁵

¹Agronomist, M.Sc, Ph.D., Professor, Graduation Program in Viticulture and Enology, Rio Grande do Sul Federal Institute, Av. Osvaldo Aranha, 540, CEP 95700-000, Bento Gonçalves, RS, Brazil

²Agronomist, M.Sc, Ph.D. Researcher, Embrapa Grape and Wine, Bento Gonçalves, RS, Brazil

³Agronomist, Postdoc, Professor, Post-graduation Program in Fitotecnia, Rio Grande do Sul Federal University, Porto Alegre, RS, Brazil

⁴Agronomist, M.Sc, Researcher, Embrapa Temperate Climate, Pelotas, RS, Brazil

⁵Chemical, Technical, Embrapa Grape and Wine, Bento Gonçalves, RS, Brazil

Abstract. The objective of this study was to characterize the photosynthetic behavior of grapevines in protected cultivation with different volumes of water available. The experiment was conducted in Vale dos Vinhedos, Brazil with covered plants of 'Italia', sustained on a discontinued pergola trellis system. The treatments consisted different available water capacity (AWC) in the soil. The control treatment (CT) was maintained at field capacity with a minimum water potential limit (ψ_m) of -33.34 kPa (100% AWC). The minimum limit of the ψ_m was -42.12 kPa (83% AWC) at T1, -76.28 kPa (53% AWC) in T2 and -94.32 kPa (30% AWC) at T3. The liquid assimilation of CO₂ (A , $\mu\text{mol CO}_2 \text{ m}^{-2} \text{ s}^{-1}$) in response to the flow density of the photosynthetically active photons ($\mu\text{mol m}^{-2} \text{ s}^{-1}$), were determined using a gas analyzer. When compared with the CT, the (A_{max}) values in T2 were 27,48% and 33% less and in T3 37,92% and 46,5% less, respectively in 2009/10 and 2010/11, while T1 didn't differ from the control. Water restrictions in covered grapevines had an influence on the foliar photosynthetic potential, with the limit of 83% AWC the most suitable condition considering the economy of water and the maintenance of foliar function.

1 Introduction

Recent studies show that a plastic covering causes alterations to some microclimatic parameters of the vegetation canopy, especially at high temperatures, with the incidence of solar radiation and wind velocity [1, 2].

The soil is both storage and a supplier of water and nutrients for plants. Through adsorption and capillarity phenomena it retains the humidity the plants need after rain or irrigation [3]. Depending on the water content in the soil, it would be easier or harder for the plants to extract it, and thus be able to meet their needs.

According to [4], under open air growing conditions, maximum cellular growth only occurs in conditions of full hydric availability, generally when the soil is in field condition ($\Psi \leq -0.03$ MPa) or when the foliar water potential is less than -0.7 Mpa. According to [2] The plastic covering does not affect the water potential on the leaf, but it reduces the demand for daily evaporation. Since it reduces the amount of solar radiation affecting

the crop, the covering reduces the evaporative demand, and thus the hydric demand of the crop [5].

According to [6], the impact of the hydric stress is more drastic when applied to the initial development of the fruit, during the initial stages of the berry (phase 1), according to the characteristic growth curve, when compared to the phases II (lag phase) and III [7]. This information might be different for table grapes where priority is given to the visual aspects such as maturation and size uniformity [8], as well as under protected crop conditions where the microclimatic variations favor the efficient use of water [2]. Under these conditions, the vines can reproduce the hydric needs during the cycle to maintain or improve the quality of the berries produced, in comparison to the conventional crop.

Despite this evidence, currently there is no characterization available for the behavior of a covered vine in relation to the variations in the irrigation depth. Therefore, it is important that there be an evaluation of the hydric deficit effects on the qualitative characteristics

^a Corresponding author: leonardo.cury@bento.ifrs.edu.br

of grapes in protected cultivation in order to create technical benchmarks for the development of effective and sustainable hydric management for this new system of vine cultivation.

2 Materials and methods

The experiment was done during the 2009/10 and 2010/11 cycles at a commercial vineyard in the Vale dos Vinhedos, Bento Gonçalves (latitude 29°12'S, longitude 51°32'W and approximate altitude of 660m). The plants used were *Vitis vinifera* L., cv. 'Itália,' six years old, grafted on rootstock '420A' and spaced 3.0m between rows and 1.8m between plants. The rows were placed in a north-south direction, conducted in a discontinuous trellis system, with mixed pruning, four stems (five buds) and 12 spurs (two buds) per plant (93 mil buds ha⁻¹). For the covering, plastic polypropylene (PP) plastic tarps were used that were braided, transparent, and impermeabilized with low density Polyethylene (160µm). To keep water entering the soil by precipitation from reaching the experimental area, gutters made from the same tarps (PP) were installed in the interrows of each experimental block, as well as the eight rows above these.

The area soil was classified as dark grey aluminic abruptic argissol with a moderate A horizon and an average/clay texture and moderate drainage. The horizons were characterized according to their morphology and subdivided according to depth. From the surface to 10cm, the horizon was classified a prominent A (Ap), from 10 to 40 cm as BA transition and from 40 to 75 cm as textural B (Bt), considering 90% of the vine root system in all of these horizons. In each horizon, three undisturbed soil samples were selected, using cylinders with a 5 cm diameter and 2.5 cm tall. The samples were saturated with distilled water and tensions of 0 kPa, saturated soil, and 1500 kPa, regarding the permanent wilting point (PWP), using a Richards' chamber [9]. According to [10], the matrix potential of the water is soil under field capacity (FC) of -33 kPa is representative of the soils with a higher clay proportion. According to [11], the agrissols represent 28.65% of the total area, distributed in 55 units of soil mapping of the Vale dos Vinhedos, which included an area of 2,327.22ha. The matrix potential data and their respective soil volumetric humidity underwent a non-linear regression analysis using the R program [12]. According to the adjusted water retention curves, the potentials equivalent to the FC and the PWP corresponded, respectively, to the volumetric humidity of 0.277 and 0.234 cm³ cm⁻³ in the Ap+BA profile, and 0.345 e 0.318cm³ cm⁻³ in Bt. With the volumetric humidity values in FC (θ_{fc}) and PWP (θ_{pwp}) and depth (Z), the available water capacity was calculated AWC (mm):

$$CAD = (\theta_{cc} - \theta_{pwp}) \cdot z \quad (1)$$

The treatments and the irrigation frequency were determined according to the available water capacity (AWC) in the horizons Ap+BA (17.2 mm) and Bt (9.45 mm). The control treatment (CT) was defined

maintaining the humidity near the FC [$\psi_m = -33.34$ kPa, 27.7% humidity in Ap+BA and 34.5% in Bt (100% of AWC)]. The soil water content was monitored by TDR (Time Domain Refractory) probes by Campbell®, model WCR CS616. After the calibration, the sensors were installed in ditches 50 cm away from the plants in the direction of the crop interrows, measuring the soil humidity in the Ap+BA and Bt horizons at 30 cm and 50 cm of depth respectively. The watering doses and the irrigation frequency were applied in such a way as to establish different levels of hydric restriction to the vines according to the crop's water consumption (evapotranspiration).

The volumetric humidity lower limit in T1 was defined as 27% in the Ap+BA horizon and 34.2% for Bt, with the AWC reduced to 83% ($\psi_m = -42,12$ kPa). In T2, the AWC was reduced to 53% with minimum humidity of 25% for Ap+BA and 33.4% for horizon Bt ($\psi_m = -76,28$ KPa). The AWC in T3 was reduced to 30%, maintaining the lower limits at 24.4% in Ap+BA and 32.8% in Bt ($\psi_m = -94,32$ KPa). When the minimum limit of the volumetric humidity was reached in each horizon (Ap+BA and Bt), the irrigation began with pre-calculated times and volumes in order to reach the FC in each one of the horizons. Considering that horizon Bt presented an elevated clay quantity and took longer to reach the considered limits, this horizon maintained the humidity of the soil for a longer period of time. At the beginning of the cycle, the irrigation was based on the volumetric humidity of the Ap+BA horizon; however, when the water available in horizon Bt reached the predetermined limit, the irrigation depth began to be calculated based on the volumetric humidity of this horizon. For the application of the irrigation depth, auto-compensating micro-sprinklers were used with a 30 L h⁻¹ flow rate, an effective radius of 1.8 m, and a ratio of 0.6 sprinklers per plant and with 40% overlap. The irrigation timing for each treatment was calculated based on the methodology proposed by [13], considering the amount of water available in each horizon, the depth (z) of each horizon, the flow rate, the effective radius of the sprinkler, and efficiency of the application per sprinkler.

With the useful plants that best represented the conditions of the vineyard, each treatment randomly marked four leaves from the canopy that were exposed to the sun with a red ribbon, with one in each block. This number of leaves per treatment was chosen due to the time available to do the analysis during a single day, without compromising the results with the photoperiodic behavior of the photosynthesis [14]. Therefore, the measurement of the gas exchanges was only done between 9:00 am and 1:00 pm, when the photosynthetic activity and the stomatal conductance are at their highest [14], in order to obtain a precise indication of the physiological responses of the vine maintained in a protected environment, under different levels of hydric deficit [15].

In the vegetative:reproductive cycles of 2009/10 and 2010/11, these leaves were submitted to the evaluation of the photosynthetic potential during the cycle in the phonological stages EF65 (full blossoming) and EF85 (start of technological maturation), according to [16]. The

$$PPFD_{sat} = \frac{-b \cdot c + b \cdot \varphi - 2A_{max} - \tau \cdot \varphi - a + M - \sqrt{(b \cdot c - b \cdot \varphi + 2 \cdot A_{max} + \tau \cdot \varphi + a - M)^2 - 4 \cdot b \cdot (c - \varphi) \cdot (2 \cdot A_{max} + \tau \cdot \varphi + a)}}{2 \cdot (c - \varphi)} \quad (7)$$

photosynthesis potential was established with a portable Infrared Gas Analyser (IRGA), Li-Cor brand, model LI-6400, Lincoln, USA, operating with a closed system, equipped with a light source model LI-6400-2B and programmed to emit levels of photosynthetically active radiation at predetermined densities.

The maximum liquid assimilation curves for CO₂ (*A*) were calculated according to the response to the photosynthetically active photon flux density (*PPFD*): 0, 100, 200, 400, 600, 800 and 1500 μmol m⁻² s⁻¹ during the 2009/10 cycle, adding the 1800, 2000, 2200 e 2500 μmol m⁻² s⁻¹ densities during the 2010/11 cycle, in accordance with the model proposed by [17] modified. According to the response curve of *A*, due to *PPFD*, the following rectangular hyperbolic function was adjusted:

$$A = -a + \frac{M \cdot x}{b + x} - c \cdot x \quad (2)$$

where *a* is the dark respiration rate (DR; μmol CO₂ m⁻² s⁻¹), *M* is a parameter related to a minimum photosynthesis rate, *b* is a parameter relating the photosynthetic quantum efficiency, and *c* is a parameter related to photo-oxidation. According to [18], the drop in the net photosynthesis rate, after reaching the radiation saturation level, can occur due to the photo-oxidation from excessive global radiation. The model used by [17] does not present the final term, which was added to consider the reduction of the photosynthesis rate under conditions of high luminous radiation levels. Through this response curve, the light compensation point (*τ*) was also figured using the value of *x* where *A* is equal to zero:

$$\tau = \frac{M - a - b \cdot c - \sqrt{(a + b \cdot c - M)^2 - 4 \cdot a \cdot b \cdot c}}{2 \cdot c} \quad (3)$$

If the model presents a *c* parameter equal to zero:

$$\tau = \frac{a \cdot b}{M - a} \quad (4)$$

The rate of maximum photosynthesis (*A_{max}*) can be calculated according to the rectangular hyperbolic model using the following formula:

$$A_{max} = M - a + b \cdot c - 2\sqrt{M \cdot b \cdot c} \quad (5)$$

The apparent quantum efficiency (*φ_a*) (μmol CO₂ μmol photons⁻¹) was estimated during the linear response curve phase of the liquid photosynthetic rate (*A*), by the slope of the tangent line to the response curve at the point where *A* is equal to zero:

$$\varphi_a = \frac{M \cdot b}{(b + \tau)^2} - c \quad (6)$$

The model recommended by [19], for the calculation of variables, does not include the calculation of saturation radiation (*PPFD_{sat}*) and the saturation photosynthesis (*A_{sat}*). Therefore, the (*PPFD_{sat}*) and (*A_{sat}*) variables were calculated based on the response curve of *A* in terms of *PPFD* of the suggested rectangular hyperbolic model. To calculate the light saturation point, initially the equation for the tangent line to the photosynthesis curve at the light compensation point was calculated. At the point where this line is equal to the maximum photosynthesis (*A_{max}*), a second line was drawn, with the opposite slant from the first. The point where this second line intercepts the photosynthesis curve was considered the saturation point by the formula 7 and 8.

$$A_{sat} = -a + \frac{M \cdot PPFD_{sat}}{b + PPFD_{sat}} - c \cdot PPFD_{sat} \quad (8)$$

All of these photosynthetic variables together characterize the photosynthetic potential and were tabled for treatment, repetition, and evaluation dates, and then were submitted to the statistical analyses using program R [12]. The data were submitted to variance (ANOVA) and to non-linear regressions analysis, and the means were compared using the Tukey test (p≤0,05).

3 Results and discussion

The larger the CO₂ consumption of the leaves, in relation to what was released by them, especially by respiration, the greater the simultaneous apparent assimilation or net photosynthesis (*A*). This variable presents itself in a different manner than the gross photosynthesis, which only specifies the total fixed CO₂. Therefore, in physiological evaluations that address photosynthesis, it is generally sufficient to know the values of the net photosynthesis to obtain the characterization of the impact of the various factors on the foliar metabolism [14]. Net photosynthesis also highlights the importance of potential assimilation response curves, estimated by a hyperbolic function, which determines the foliar response capacity in different simulated conditions of photosynthetically active radiation. In these same curves, it is possible to obtain different variables simultaneously, such as dark respiration, (*DR*), compensation point (*τ*), quantum efficiency (*φ_a*), saturation radiation (*PPFD_{sat}*), saturation photosynthesis (*A_{sat}*) and maximum photosynthesis (*A_{max}*), which are important tools to characterize the photosynthetic responses of the leaves in the specific environmental condition.

In the analysis of photosynthetic variables in the full flowering stage, it is worth highlighting that, during both cycles, the hydric restriction imposed by the 30% AWC treatment was sufficient to alter the dark respiration rate (*Re*), reaching 1.76 and 1.63 μmol CO₂ m⁻² s⁻¹,

^a Corresponding author: leonardo.cury@bento.ifrs.edu.br

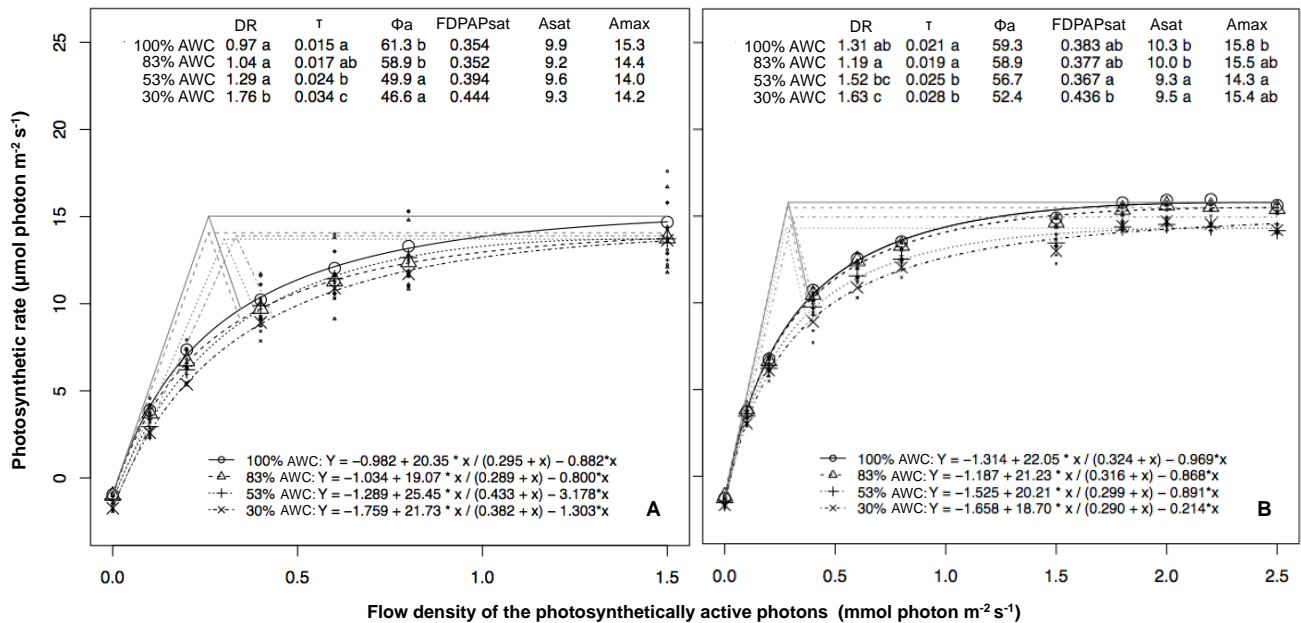


Figure 1. CO₂ assimilation 2009/10 (A) and 2010/11 (B) due to the increase of the photosynthetically active photon flux density (PPFD) in grapevines 'Italy' grown in protected cultivation, under different treatments of water restriction, in the full flowering stage (EF65) [16]. In net photosynthesis tables, the mean photosynthetic variables dark respiration (DR), compensation point (τ), quantum efficiency (Φ_a), photosynthetic saturation photons flux (PPFD_{sat}), photosynthesis saturation (Asat) and maximum photosynthesis (Amax) followed by the same letter do not differ by Tukey test ($p \leq 0,05$). Bento Gonçalves, RS, 2012.

respectively, in the 2009/10 and 2010/11 cycles. In relation to the CT, these values represent a respiratory increase of $0.79 \mu\text{mol CO}_2 \text{ m}^{-2} \text{ s}^{-1}$ ($P=0.002$) in 2009/10 and $0.44 \mu\text{mol CO}_2 \text{ m}^{-2} \text{ s}^{-1}$ ($P<0.0001$) in 2010/11 (Figure 1). This increase in the release of CO₂ in the dark highlights the unfavorable conditions for the assimilation and/or increase of the tissue maintenance metabolism in these conditions of hydric stress.

As a result of this increase in the rate of dark respiration, the 30% AWC treatment also imposed an alteration of the light compensation point (τ) in the 2009/10 cycle. This variable was significantly increased by $19.44 \mu\text{mol photons m}^{-2} \text{ s}^{-1}$ ($P<0.0001$) when compared to TC, reaching a value of $34.48 \mu\text{mol photons m}^{-2} \text{ s}^{-1}$ (Figure 1).

Analyzing the 2010/11 cycle, one realizes that the radiation regarding the light compensation point in both treatments is increased significantly with greater hydric restriction (T2 and T3), reaching respective values of 24.82 and $28.32 \mu\text{mol photons m}^{-2} \text{ s}^{-1}$ (Figure 1). In relation to T1, this increase reached $5.83 \mu\text{mol photons m}^{-2} \text{ s}^{-1}$ ($P = 0.003$) and $9.33 \mu\text{mol photons m}^{-2} \text{ s}^{-1}$ ($P < 0.0001$), respectively. Although these values are lower, compared to 2009/10, they clearly demonstrate that the increase in respiratory rate for treatments with a larger soil hydric deficit imposes higher demand for light to reach the compensation point. This is typical behavior of C₃ plants such as the vine, showing τ elevations in conditions of light, water, or nutrition restrictions and temperature increases [20].

Changes in the photosynthetic rate observed in full bloom are accentuated in the evaluations at the beginning of the technological maturation (EF85) [16] as a result of

the longer time under hydric stress imposed by the irrigation treatments.

The matrix potential of water in the lower soil for horizon BA and Bt, in the T2 and T3 treatments, induced hydric stress in T2 and a more intense stress in T3, clearly evidenced by the significant increase in dark respiration (DR), in comparison to the control (100% CAD) (Figure 2). These differences in comparison to the control reached similar values in both cycles, with 0.64 ($P < 0.0001$) and $0.86 \mu\text{mol CO}_2 \text{ m}^{-2} \text{ s}^{-1}$ ($P < 0.0001$), respectively during 2009/10, and 0.66 ($P < 0.0001$) and $0.86 \mu\text{mol CO}_2 \text{ m}^{-2} \text{ s}^{-1}$ ($P < 0.0001$) during 2010/11 (Figure 2).

The restoration of the photosynthetic capacity in vines that underwent the intense hydric deficits imposed on T2 and T3 can be reached a few hours [21], and up to five days [22], after application of the irrigation depth, depending on the intensity and length of time of the hydric stress imposed on plants. Therefore, as these stress conditions were imposed throughout the growing cycle, the plants adopted more robust tolerance mechanisms, such as morphological and osmotic adjustments, in order to maintain photosynthetic activities during these stress conditions.

As a result of this increase in the respiratory rate, it is worth emphasizing that the plants grown in these treatments increased the need for light to reach the compensation point (τ), recording respective values of 34.71 and $33.63 \mu\text{mol photons m}^{-2} \text{ s}^{-1}$ during the 2009/10 and 32.61 and $35.23 \mu\text{mol photons m}^{-2} \text{ s}^{-1}$ during 2010/11 (Figure 2).

Comparing the plants grown in 53% and 30% AWC compared to control, an increase in light intensity of

^a Corresponding author: leonardo.cury@bento.ifrs.edu.br

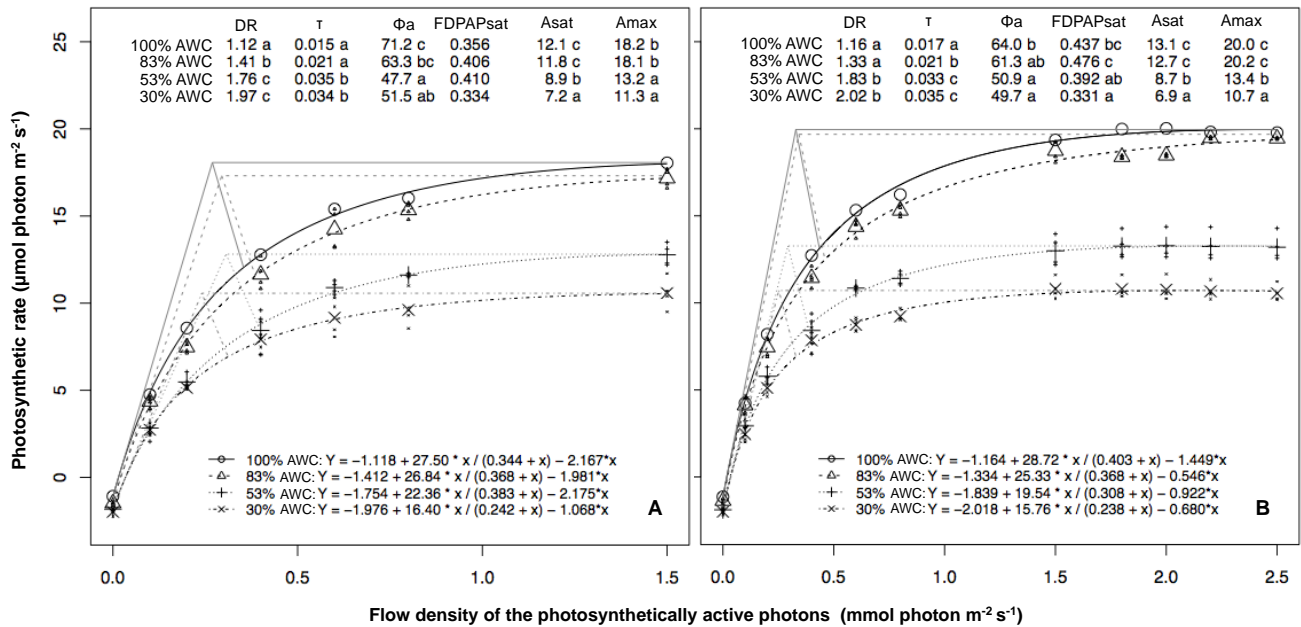


Figure 2. CO₂ assimilation 2009/10 (A) and 2010/11 (B) due to the increase of the photosynthetically active photon flux density (PPFD) in grapevines 'Italy' grown in protected cultivation, under different treatments of water restriction, in the beginning of the technological maturation (EF85) [16]. In net photosynthesis tables, the mean photosynthetic variables dark respiration (DR), compensation point (τ), quantum efficiency (Φ_a), photosynthetic saturation photons flux (PPFD_{sat}), photosynthesis saturation (Asat) and maximum photosynthesis (A_{max}) followed by the same letter do not differ by Tukey test ($p \leq 0,05$). Bento Gonçalves, RS, 2012.

19.68 ($P < 0.0001$) and 18.67 $\mu\text{mol photons m}^{-2} \text{s}^{-1}$ ($P = 0.001$) during 2009/10 and 15.27 ($p < 0.0001$) and 18.10 $\mu\text{mol photons m}^{-2} \text{s}^{-1}$ ($P < 0.0001$) in 2010/11 were observed, showing the state of stress imposed by treatments that applied higher water deficits.

After the leaf reaches the light compensation point, the absorption of CO₂ increases linearly until it reaches a saturation point. Therefore, in this linear phase there is a direct proportionality between the availability of radiation and the photosynthetic yield, where the capture capacity and the incident radiation processing (photochemical stage of photosynthesis) is the determination point for the photosynthetic responses. In other words, the larger the quantum gain (Φ_a), the greater the slope will be during the linear phase of the net photosynthesis curve due to the radiation (apparent quantum efficiency (Φ_a), expressed in moles of CO₂ per incident photon mol).

Therefore, a higher slope of the linear phase of the curve represents a larger CO₂ fixation with less expenditure of light photons. When this increase in the CO₂ fixation reaches the maximum limit (end of the linear phase), the biochemical step of photosynthesis (Ribulose - 1,5 - biphosphate carboxylase/oxygenase enzyme activity \times CO₂ concentration) is what becomes the limiting factor.

The point where photosynthesis becomes invariable to an increase in radiation, corresponds to the flow density level of photosynthetic saturation photons (PPFD_{sat}). In this context, the apparent quantum efficiency and the PPFD_{sat}, along with R_e and τ , are directly influenced by environmental conditions and will vary according to the plant species.

In the contrast between the irrigation treatments, it is emphasized that, throughout the cycle, the most drastic

hydic restrictions imposed by T2 and T3 yielded a reduction in the slope of the tangent line of photosynthetic growth, in relation to available radiation, significantly reducing the apparent quantum efficiency (ϕ_a) compared to T1 and TC treatments.

This effect was noticed at the full bloom stage in 2009/10, when the leaves were not fully expanded, reaching average values of 49.92 and 46.62 $\text{nmol CO}_2 \text{m}^{-2} \text{s}^{-1} / \mu\text{mol photons m}^{-2} \text{s}^{-1}$ respectively (Figure 1). At this time, the reduction of the quantum efficiency in regard to the 100% AWC treatment was 23.43% ($P = 0.009$) and 19.67 $\text{nmol CO}_2 \text{m}^{-2} \text{s}^{-1} / \mu\text{mol photons m}^{-2} \text{s}^{-1}$ ($P = 0.002$) respectively, at T2 and T3.

These results highlight that, even in the early stages of the phenological cycle, the hydic restriction conditions have already caused photosynthetic changes during the photochemical phase, as pointed out by other authors [23,17]. However, despite significant effects on the quantum yield, the contrasts of hydic availability in the full bloom of the 2009/10 cycle were not sufficient to influence the maximum photosynthesis (A_{max}) and the photosynthetic saturation photons flux (PPFD_{sat}), significant only in 2010/11 cycle (Figure 1).

Thus, one can assume that the variable ϕ_a is more sensitive when characterizing the effects of hydic restriction to the vine and predates more drastic effects, such as pigment and protein degradation, which limit photosynthetic capacity during prolonged periods of hydic stress [14].

However, when analyzing the 2010/11 cycle during the full flowering stage, the ϕ_a variable showed no significant differences between treatments. That year, it was also observed that T3, while there were no changes in the quantum efficiency, the saturation radiation

^a Corresponding author: leonardo.cury@bento.ifrs.edu.br

increased by 68.86 $\mu\text{mol photons m}^{-2} \text{s}^{-1}$ ($P = 0.09$) with respect to T1, and that T2 as well as T3 reduced the photosynthesis saturation by 0.98 and 0.79 $\mu\text{mol CO}_2 \text{ m}^{-2} \text{s}^{-1}$ in comparison to TC (Figure 1).

Only after moving forward in the vegetative production cycle, with a longer exposure of the plants to different hydric conditions and with greater foliar maturity, could the contrast between the variables be seen clearly. At the beginning of the technological maturity of the berries (EF85) [16], the T2 and T3 treatments can be observed to have promoted a more intense and significant reduction of the apparent quantum efficiency (ϕ_a) in comparison to the other treatments (Figure 2).

This behavior demonstrates an underutilization of photons in the photochemical phase for these more stressful conditions, possibly because they have less integrity and a lower amount of photosynthetic apparatus. According to [24], healthy leaves that have not been subjected to stress exhibit apparent quantum efficiency between 60 and 75 $\text{CO}_2 \text{ m}^{-2} \text{s}^{-1} / \mu\text{mol photons m}^{-2} \text{s}^{-1}$, which is equivalent to the values found in TC (71.19 $\text{nmol CO}_2 / \mu\text{mol photons}$ in 2009/10, and 64.04 $\text{nmol CO}_2 / \mu\text{mol photons}$, in 2010/11) and T1 (63.32 $\text{nmol CO}_2 / \mu\text{mol photons}$ in 2009-10, and 61.25 $\text{nmol CO}_2 / \mu\text{mol photons}$, in 2010/11), during this phenological stage (Figure 2).

At this stage the contrasts in maximum photosynthesis (A_{max}) and photosynthesis saturation (A_{sat}) also stood out, even though there was no significant difference in saturation radiation (Figure 2). In these contrasts, the treatments that underwent more intense hydric deficits (T2 and T3) had the lowest values of A_{max} and A_{sat} , with the most dramatic responses in T3 (Figure 2).

According to [25], leaf ontogeny is subdivided into three phases of photosynthetic use, matching the physiological steps of the foliar age. In TC and T1, exposed to levels of less intense hydric stress during the cycle, photosynthesis reached values of 18.15 $\mu\text{mol CO}_2 \text{ m}^{-2} \text{s}^{-1}$ and 18.10 $\mu\text{mol CO}_2 \text{ m}^{-2} \text{s}^{-1}$, in 2009/10 and 19.95 $\mu\text{mol CO}_2 \text{ m}^{-2} \text{s}^{-1}$ and 20.17 $\mu\text{mol CO}_2 \text{ m}^{-2} \text{s}^{-1}$, 2010/11, respectively (Figure 2).

Considering that the maximum photosynthesis in the vine is achieved when the leaves reach their maximum morphological development, occurring 30-40 days after splitting from the apex, remaining at maximum capacity for two to four weeks [26], one can state that these maximum values were achieved in both analysis cycles.

This is in agreement with [27,28], which state that under a lack of hydric stress, maximum photosynthetic activity is stimulated when demand for carbohydrates is high, such as during the period of berry enlargement and the intense sprouting.

Furthermore, it should be noted that vines maintained under protected cultivation, in which photosynthesis is favored by the reduced vapor pressure deficit and increased stomatal conductance [2], along with the treatments where there is no hydric deficit (TC) or when it is at a minimum (T1), gas exchange are favored, thus increasing the water use efficiency.

Comparing these maximum photosynthesis values with the values obtained in more limited water conditions, the treatment maintained at 30% AWC

promoted photosynthetic reductions of 37.85% and 47.93% in the respective cycles. According to [14], the maximum rates of net photosynthesis during a period of hydric stress are 20% to 66% lower than in normal hydric conditions. The main explanation for this reduction in photosynthetic capacity is the reduction in stomatal conductance.

The general data observation of gas exchanges throughout the cycle show that the reduction of atmospheric evaporative demand imposed by the protected cultivation favored the extension of foliar biochemical functions and the exchange of gases, and maintaining soil humidity at field capacity was not necessary (100% AWC).

The light hydric stress imposed on plants kept at 83% AWC was not able to significantly alter the foliar functions, maintaining high photosynthesis levels, allowing the sustainable use of hydric resources.

4 Conclusion

According to the experimental conditions the plastic covering promoted microclimatic alterations, which altered the hydric necessity of the vine and increase the efficiency of water use.

The hydric restriction in covered vineyards influenced the foliar photosynthetic potential, where a limit of 83% AWC was the most appropriate condition when considering the water savings and the maintenance of the foliar function.

References

1. L.S. Cardoso, H. Bergamaschi, F. Comiran, G. Chavarria, G.A.B. Marodin, G.A. Dalmago, H.P. Santos, F. Mandelli. Alterações micrometeorológicas em vinhedos pelo uso de coberturas de plástico. *Pesqu. Agropec Bras.*, **43**, 441-447 (2008)
2. G. Chavarria, H.P. Santos, J. Felippeto, G.A.B. Marodin, H. Bergamaschi, L.S. Cardoso, F.B. Fialho. Relações hídricas e trocas gasosas em vinhedo sob cobertura plástica. *Rev. Bras. Frut.*, **30**, 1022-1029 (2008)
3. H. Bergamaschi, M.A. Berlato, R. Matzenauer, D.C. Fontana, G.R. da Cunha, M.L.V. Santos, J.R.B. Farias, N.A. Barni. *Agrometeorologia aplicada à irrigação*, UFRGS, 125p (1999)
4. G.F. Gil, P. Pszczólkowski. *Viticultura: Fundamentos para optimizar producción y calidad*, UCC, 535p (2007)
5. V.L. Barradas, E. Nicolás, A. Torrecillas, J.J. Alarcón. Transpiration and canopy conductance in Young apricot (*Prunus armenica* L.) trees subjected to different PAR levels and water stress. *Agric. Water Manag.*, **77**, 323 -333 (2005)
6. J. Kennedy. Understanding grape berry development. *Pract. Wine. Vine. J.*, **2**, 14-23 (2002)
7. L.E. Williams, L.E. Trout. Relationship among vine-and-soil-based measures of water status in a Thompson Seedless vineyard in response to high-

- frequency drip irrigation. *Am. J. Enol. Vitic.*, **56**, 357-366 (2005)
8. C. Padilla, P. Villalobos, A. Spiller, G. Henry. Consumer preference and willingness to pay for an officially certified quality label: implications for traditional food producers. *Agric. Téc.*, **67**, 300-308 (2007)
 9. A. Klute. Water retention: laboratory methods. *Methods of soil analysis: physical and mineralogical methods*. Am. Soc. Agron., 635-662 (1986)
 10. H.A. Ruiz, G.B. Ferreira, J.B.M. Pereira. Estimativa da capacidade de campo de latossolos e neossolos quartzarênicos pela determinação do equivalente de umidade. *Rev. Bras. Ciên. Solo*, **27**, 389-393 (2003)
 11. C.A. Flores, R.O. Pötter, E.C. Sarmento, E.J. Weber, H. Hasenack. Os solos do Vale dos Vinhedos. Embrapa, 216p. (2012)
 12. R Development Core Team. R: A language and environment for statistical computing. R Foundation for Statistical Computing (2014)
 13. M.A.F. Conceição. Sistema de produção de uva de mesa do Norte de Minas Gerais. Embrapa (2005)
 14. W. Larcher. *Physiological plant ecology*. 513p. (2004)
 15. H. Medrano, J.M. Escalona, J. Cifre, J. Bota, J. Filexas. A ten-year study on the physiology of two Spanish grapevine cultivars under field conditions: effects of water availability from leaf photosynthesis to grape yield and quality. *Func. Pl. Bio.* **30**, 607-619 (2003)
 16. D.H. Lorenz, K.W. Eichorn, H. Bleholder, R. Klose, U. Meier, E. Weber. Phenological growth stages of grapevine (*Vitis vinifera* L.) - Codes and descriptions according to the extended BBCH scale. *Aust. J. Grap. Win. Res.*, **1**, 100-103 (1995)
 17. C.S. Mota, C.V.T. Amarante, H.P. Santos, J.A. Albuquerque. Disponibilidade hídrica, radiação solar e fotossíntese em videiras ‘Cabernet Sauvignon’ sob cultivo protegido. *Rev. Bras. Frut.*, **31**, 432-439 (2009)
 18. M. Kitao, T.T. Lei, T. Koike, H. Tobita, Y. Maruyama. Susceptibility to photoinhibition of three deciduous broadleaf tree species with different successional traits raised under various light regimes. *Pl., Cel. Env.*, **23**, 81-89 (2000)
 19. T.C. Platt, C.L. Gallegos, W.G. Harrison. Photoinhibition of photosynthesis in natural assemblages of marine phytoplankton. *J. Mar. Res.* **38**, 687-701 (1980)
 20. H. Bauer, P. Martha, B. Kirchner-Heiss, I. Mairhofer. The CO₂ compensation point of C₃ plants a re-examination. II. Intraspecific variability. *Z. Pflanz.*, **109**, 143-154 (1983)
 21. W.T. Liu, R. Pool, W. Wenkert, P.E. Kriedemann. Changes in photosynthesis, stomatal resistance and abscisic acid of *Vitis labruscana* through drought and irrigated cycles. *Am. J. Enol. Vitic.*, **29**, 239-246 (1978)
 22. A. Scienza, M. Fregoni, M. Boselli. Influenza del portinnesto sulla resistenza stomatica, sul potenziale idrico e sul contenuto di acido abscísico di foglie di “Barbera”. *Vign.*, **1**, 39-44 (1980)
 23. M. Pessaraki. *Handbook of photosynthesis*, CRC Press, 928 p. (2005)
 24. H.R. Bolhàr-Nordenkamp, S.P. Long, N.R. Baker, G. Öquist, U. Shureiber, E.G. Lechner. Chlorophyll fluorescence as probe of the photosynthetic competence of leaves in the field: a review of current instrumentation. *Func. Ecol.*, **3**, 497-514 (1989)
 25. J. Catsky, Z. Sesták. Photosynthesis during leaf development. *Handbook of photosynthesis*. 633-660 (1997)
 26. M. Bertamini, N. Nedunchezian. Photoinhibition of photosynthesis in mature and young leaves of grapevine (*Vitis vinifera* L.) *Pl. Sci.*, **164**, 635-644 (2003)
 27. D. Iglesias, F.R. Tadeo, E. Primo-Millo, M. Talón. Fruit set dependence on carbohydrate availability in citrus trees. *Tree Phys.*, **23**, 199-204 (2003)
 28. R.V. Ribeiro, E.C. Machado. Some aspects of citrus ecophysiology in subtropical climates: re-visiting photosynthesis under natural conditions. *Braz. J. Plan. Phys.*, **19**, 393-411 (2007)